Molecular Cell
Article

Sirt3-Mediated Deacetylation of Evolutionarily Conserved Lysine 122 Regulates MnSOD Activity in Response to Stress

Randa Tao,[1,8] Mitchell C. Coleman,[2,8] J. Daniel Pennington,[1] Ozkan Ozden,[4,5] Seong-Hoon Park,[4,5] Haiyan Jiang,[4,5] Hyun-Seok Kim,[4,5] Charles Robb Flynn,[6] Salisha Hill,[7] W. Hayes McDonald,[7] Alicia K. Olivier,[3] Douglas R. Spitz,[2] and David Gius[4,5,*]

[1]Howard Hughes Medical Institute and Molecular Radiation Oncology, Radiation Oncology Branch, Center for Cancer Research, NCI, NIH, Bethesda, MD 20892, USA
[2]Free Radical and Radiation Biology Program, Department of Radiation Oncology, Holden Comprehensive Cancer Center
[3]Department of Pathology, Carver College of Medicine
University of Iowa, Iowa City, IA 52242, USA
[4]Department of Radiation Oncology
[5]Department of Pediatrics
Vanderbilt University Medical Center, Nashville, TN 37232, USA
[6]Department of Surgery
[7]Mass Spectrometry Research Center
VanderbiltUniversity School of Medicine, Nashville, TN 37232, USA
[8]These authors contributed equally to this work
*Correspondence: david.gius@vanderbilt.edu
DOI 10.1016/j.molcel.2010.12.013

SUMMARY

Genetic deletion of the mitochondrial deacetylase sirtuin-3 (*Sirt3*) results in increased mitochondrial superoxide, a tumor-permissive environment, and mammary tumor development. MnSOD contains a nutrient- and ionizing radiation (IR)-dependent reversible acetyl-lysine that is hyperacetylated in Sirt3$^{-/-}$ livers at 3 months of age. Livers of Sirt3$^{-/-}$ mice exhibit decreased MnSOD activity, but not immunoreactive protein, relative to wild-type livers. Reintroduction of wild-type but not deacetylation null *Sirt3* into Sirt3$^{-/-}$ MEFs deacetylated lysine and restored MnSOD activity. Site-directed mutagenesis of MnSOD lysine 122 to an arginine, mimicking deacetylation (lenti-MnSOD$^{K122\text{-}R}$), increased MnSOD activity when expressed in MnSOD$^{-/-}$ MEFs, suggesting acetylation directly regulates function. Furthermore, infection of Sirt3$^{-/-}$ MEFs with lenti-MnSOD$^{K122\text{-}R}$ inhibited in vitro immortalization by an oncogene (*Ras*), inhibited IR-induced genomic instability, and decreased mitochondrial superoxide. Finally, IR was unable to induce MnSOD deacetylation or activity in Sirt3$^{-/-}$ livers, and these irradiated livers displayed significant IR-induced cell damage and microvacuolization in their hepatocytes.

INTRODUCTION

The incidence of human malignancies increases exponentially as a function of age, suggesting a mechanistic connection between aging and carcinogenesis (Finkel et al., 2009). Mammalian cells contain tumor suppressor (TS) genes, such as p53, and loss of TS function results in a damage-permissive phenotype (Sherr and McCormick, 2002) that is an early event in carcinogenesis. *Sirt3* is one of three sirtuins localized to mitochondria (Onyango et al., 2002; Schwer et al., 2002) and is the primary mitochondrial protein deacetylase (Lombard et al., 2007). Since cancer is a disease of aging and sirtuin genes appear to defend against cellular damage during aging, it has been proposed that *Sirt3* plays an anticarcinogenic role and functions as a TS protein (Kim et al., 2010).

Mitochondria are thought to be central to aging, and the correct function of mitochondria impedes the processes of aging and carcinogenesis by tightly regulating the reactive oxygen species generated as a byproduct of normal respiration activities (Singh, 2006). Mitochondrial abnormalities associated with altered oxidative metabolism are observed in tumor cells in vitro and in vivo and appear to contribute to a chronic condition of oxidative stress (Aykin-Burns et al., 2009). One intriguing finding from our previous work demonstrated that cells lacking *Sirt3* exhibited altered metabolism, including a significant increase in mitochondrial superoxide levels when exposed to IR. In this regard, manganese superoxide dismutase (MnSOD) is the primary mitochondrial scavenging enzyme that converts superoxide to hydrogen peroxide, which is subsequently converted to water by catalase (Spitz and Oberley, 1989). Since MnSOD enzymatically scavenges superoxide, which is increased in irradiated cells lacking *Sirt3* (Kim et al., 2010), it seemed logical to suggest that cells lacking *Sirt3* might have altered regulation of MnSOD.

Sirt3 knockout mice develop invasive ductal mammary tumors, and Sirt3$^{-/-}$ mouse embryonic fibroblasts (MEFs) are easily immortalized and transformed by infection of a single oncogene (Kim et al., 2010). SIRT3 levels are also decreased in human breast malignancies as compared to normal breast

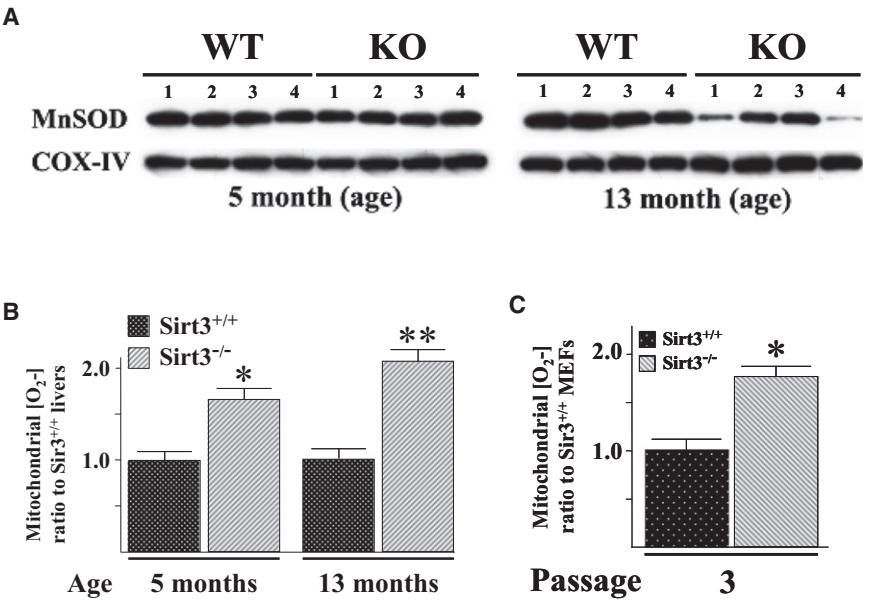

Figure 1. MnSOD Protein and Superoxide Levels in *Sirt3* Wild-Type and Knockout Mouse Livers and MEFs

(A) Livers from four Sirt3$^{+/+}$ and Sirt3$^{-/-}$ mice at 5 and 13 months of age were harvested, and mitochondrial extracts were made. Lysates were separated by SDS-PAGE, transferred onto nitrocellulose, and processed for immunoblotting with an anti-MnSOD antibody (Santa Cruz Biotechnology, Inc.; Santa Cruz, CA).

(B) Mitochondrial superoxide levels, assessed using MitoSOX oxidation, were determined in the *Sirt3* wild-type and knockout mouse livers at 5 and 13 months of age. Superoxide levels were measured as previously described.

(C) Mitochondrial superoxide levels were determined in wild-type and Sirt3$^{-/-}$ MEFs using MitoSOX oxidation at culture passage number three, as previously described (Kim et al., 2010). Results in this figure are the mean of at least three separate experiments. Error bars represent one standard deviation. * indicates $p < 0.05$ and ** indicates $p < 0.01$ by t test.

tissues, as well as in several other human malignancies (Kim et al., 2010), suggesting that *Sirt3* is a nuclear-encoded, mitochondria-localized TS. A biochemical examination of the in vitro transformed Sirt3$^{-/-}$ MEFs, as well as murine tumors, strongly suggested a potential connection between aberrant mitochondrial superoxide levels and a transformation/tumor-permissive cell phenotype. Specifically, a statistically significant decrease in mitochondrial MnSOD protein levels was observed at roughly 1 year that corresponded with the first incidence of murine mammary tumors (Kim et al., 2010). In addition, MnSOD transcription, via a mechanism involving decreased FOXO3a acetylation, was shown to decrease at roughly the same time that the first tumors were observed in the *Sirt3* knockout mice. Finally, viral overexpression of *MnSOD* prevented in vitro immortalization and transformation of the Sirt3$^{-/-}$ MEFs by an oncogene as well as preventing IR-induced increases in mitochondrial superoxide levels, further suggesting a role of MnSOD in the carcinogen-permissive phenotype observed in cells lacking *Sirt3*.

However, if increased mitochondrial superoxide levels play a role in carcinogenesis, it would seem logical that the decrease in MnSOD protein/activity would occur at a time point earlier than 1 year when it was observed that mammary tumors begin to appear in the Sirt3$^{-/-}$ animals. Thus, while the mechanistic connection between the Sirt3$^{-/-}$ mouse in vivo tumor-permissive phenotype and increased mitochondrial superoxide seemed strong, the definition of its role as an early event in carcinogenesis seemed incomplete. Thus, we proposed that Sirt3 might regulate mitochondrial superoxide levels via a second mechanism that occurs much earlier than 1 year and is independent of total mitochondrial MnSOD protein levels. If this is the case, then loss of *Sirt3* might also result in decreased MnSOD enzymatic activity by a posttranslational mechanism, presumably via protein/lysine acetylation, which might account for the aberrant increase in mitochondrial superoxide levels, while mitochondrial MnSOD protein levels remain unchanged.

RESULTS

The Kinetics of MnSOD Protein Levels Do Not Correlate with Mitochondrial Superoxide Levels

The *Sirt3* knockout mice develop tumors beginning at roughly 13 months, and these tumors, as well as the in vitro transformed MEFs, exhibit significant aberrant mitochondrial metabolism, including elevated superoxide levels (Kim et al., 2010). In this regard, a decrease in MnSOD transcription and mitochondrial MnSOD protein is also observed between 9 and 13 months in the *Sirt3* knockout mice, as compared to the wild-type mice (Figures 1A and S1A). Interestingly, mitochondrial superoxide levels are significantly increased in the livers of Sirt3$^{-/-}$ mice at 5 months of age (Figure 1B), when the levels of mitochondrial MnSOD protein in the *Sirt3* wild-type and knockout mice are identical (Figure 1A).

Mitochondrial superoxide levels were also increased in Sirt3$^{-/-}$ MEFs at passage three, as compared to the Sirt3$^{+/+}$ MEFs (Figure 1C), while MnSOD levels are identical (Figure S1B). No changes in catalase activity (Figure S1C) or catalase protein levels were observed between these mice (Figure S1D). Thus, these results suggested that Sirt3 may be involved in the regulation, at least in part, of mitochondrial superoxide levels via a mechanism involving a posttranslational modification of MnSOD. Since Sirt3 is the primary mitochondrial lysine deacetylase (Lombard et al., 2007), it seemed reasonable to propose that Sirt3 may regulate MnSOD enzymatic dismutase activity via changes in MnSOD lysine acetylation.

MnSOD Contains a Reversible Acetyl-Lysine, and MnSOD Activity Is Decreased in Sirt3$^{-/-}$ Cells

Evidence that MnSOD contains reversibly acetylated lysine residues was obtained when wild-type mice at 3 months of age were fasted for 36 hr and liver extracts were harvested, immunoprecipitated (IPed) with an anti-MnSOD antibody, separated into

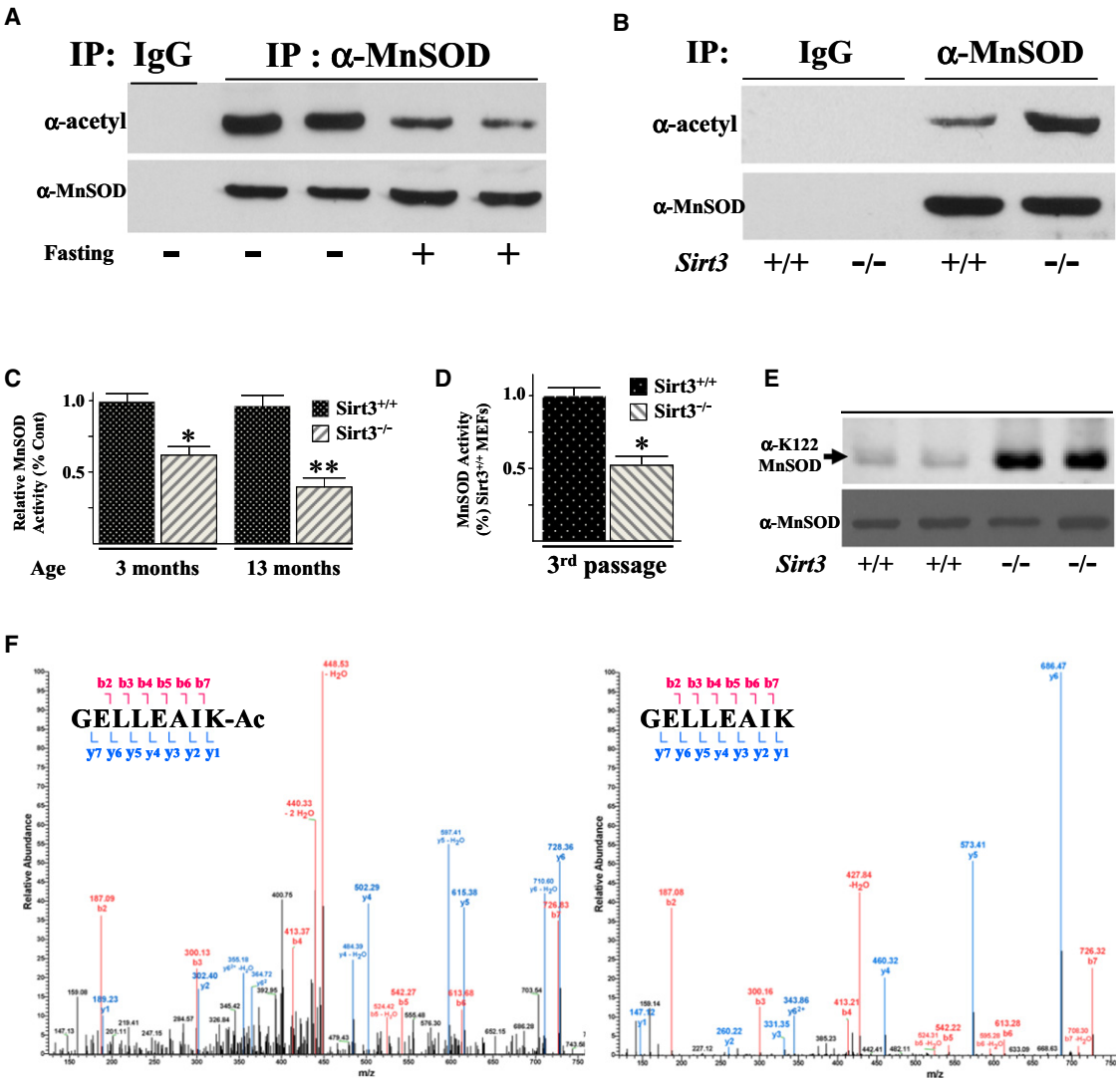

Figure 2. MnSOD Contains a Reversibly Acetylated Lysine Residue, and Protein Deacetylation and SOD Activity Are Decreased in *Sirt3*$^{-/-}$ Cells

(A) Isogenic, 3-month-old, age-matched Sirt3$^{+/+}$ mice were fasted for 36 hr, and livers were harvested, IPed with an anti-MnSOD antibody (Santa Cruz Biotechnology, Inc.), separated into two equal fractions, and subsequently immunoblotted with an anti-acetyl (Abcam; Cambridge, MA) or anti-MnSOD antibody.

(B) Livers from isogenic, 3-month-old, age-matched Sirt3$^{+/+}$ and Sirt3$^{-/-}$ mice were harvested, IPed with an anti-MnSOD antibody, separated into two equal fractions, and immunoblotted with either an anti-acetyl or anti-MnSOD antibody. Representative gels are shown for (A) and (B).

(C and D) MnSOD activity in *Sirt3* wild-type and knockout mouse livers at 3 and 13 months of age (C) and MEFs at passage number three (D). MnSOD activity was measured via a competitive inhibition assay as described (Spitz and Oberley, 1989). Activity data for MnSOD are presented as units of SOD activity per milligram of protein. Results in this figure are the mean of at least three separate experiments. Error bars represent one standard deviation. * indicates $p < 0.05$ and ** indicates $p < 0.01$ by t test.

(E) Livers from isogenic, 3-month-old, age-matched Sirt3$^{+/+}$ and Sirt3$^{-/-}$ mice were harvested and immunoblotted with an anti-K122-MnSOD antibody (Epitomics, Inc.; The Rabbit Monoclonal Antibody Company) recently produced for the laboratory.

(F) Tandem mass spectrometry from MnSOD demonstrates acetylated lysine 122 in vivo. Liver mitochondria from wild-type and Sirt3$^{-/-}$ mice were resolved by SDS-PAGE, followed by in-gel trypsin digestion, separation by nanoscale reverse-phase chromatography on reverse-phase columns, and analysis by OrbiTrap analyzer via an electrospray interface. See Supplemental Experimental Procedures for complete description. The spectrum represents the fragmentation of the m/z ratios of the MnSOD peptide sequences GELLEAIK (+2 charge = 436.7580 monoisotopic mass) and GELLEAIK-ac (+2 charge = 457.7633 monoisotopic mass).

equal fractions, resolved, and then immunoblotted with either an anti-acetyl (Figure 2A, upper panel) or anti-MnSOD antibody (lower panel). These experiments showed a decrease in acetylated MnSOD (Figure 2A, upper panel), while IPed MnSOD (lower panel) and total mitochondrial MnSOD protein levels were similar (Figure S2A). In addition, no difference in MnSOD protein acetylation (Figure S2B, upper panel), IPed MnSOD (lower panel), or total mitochondrial MnSOD protein (Figure S2C, lane 1 versus 3)

was observed in the livers of the Sirt3$^{-/-}$ mice at 3 months of age or when these mice were fasted, as compared to the fed mice.

Livers from isogenic, 3-month-old, age-matched wild-type and Sirt3$^{-/-}$ mice were also harvested, IPed with an anti-MnSOD antibody, separated into two equal fractions, resolved, and immunoblotted with either an anti-acetyl (Figure 2B, upper panel) or anti-MnSOD antibody (lower panel). These results showed that MnSOD acetylation was increased in the Sirt3$^{-/-}$ livers (Figure 2B), while no difference in total MnSOD (lower panel) or mitochondrial MnSOD (Figure S2C, lane 1 versus 2) was observed. Nicotinamide phosphoribosyl transferase (NAMPT) enhances cellular NAD levels and increases Sirt1 transcriptional activity in a dose-dependent manner (Revollo et al., 2004), so it seemed reasonable to determine if NAMPT levels are increased in our fasting mice and whether this induces Sirt3. Liver samples from the Sirt3$^{+/+}$ or Sirt3$^{-/-}$ mice, with and without fasting, were immunoblotted with an anti-NAMPT antibody, and no change in NAMPT levels was observed (Figure S2D).

These results support the hypothesis that MnSOD is a target for reversible lysine acetylation mediated by Sirt3. Thus, MnSOD enzymatic activity was determined in the *Sirt3* knockout livers as well as MEFs, and these results showed that MnSOD activity was significantly decreased in liver tissues from Sirt3$^{-/-}$ mice at age 3 months and Sirt3$^{-/-}$ MEFs at passage number three (Figures 2C and 2D). Total MnSOD levels were similar in the Sirt3$^{-/-}$ livers (Figure S2C), as compared to the Sirt3$^{+/+}$ liver controls. In addition, immunoblotting with an anti-acetyl-lysine 122 MnSOD (Epitomics, Inc.; Burlingame, CA) antibody (Figure 2E) as well as mass spectrometry (Figures 2F and S2E) demonstrated an increase in the acetylation of MnSOD lysine 122 in the liver samples from Sirt3$^{-/-}$ mice at 3 months of age, as compared to age-matched wild-type mice.

Re-Expression of Sirt3 Deacetylates MnSOD and Restores Superoxide Dismutase Activity

To determine if Sirt3 directly deacetylates MnSOD and alters enzymatic activity, two lentiviruses were constructed that expressed either the wild-type (lenti-Sirt3-WT) or a deacetylation null mutant (lenti-Sirt3-DN) *Sirt3* gene (a gift from Toren Finkel, NHLBI) in which amino acid 248 was changed from histidine to tyrosine (Ahn et al., 2008). These viruses were used to infect Sirt3$^{-/-}$ MEFs. Infection with lenti-Sirt3-WT, but not lenti-Sirt3-DN, decreased MnSOD acetylation (Figure 3A, lane 3 versus 4, upper panel), while infection of these lentiviruses expressed similar levels of exogenous Sirt3 wild-type and mutant protein (Figure 3B). Lenti-Sirt3-WT, but not lenti-Sirt3-DN, also increased MnSOD activity (Figure 3C) and decreased mitochondrial superoxide levels (Figure 3D), while the levels of IPed MnSOD were similar in the control and infected Sirt3$^{-/-}$ MEFs (Figure 3A, lower panel). These results support the hypothesis that Sirt3 directly deacetylates MnSOD, leading to increased dismutase activity.

To more rigorously determine if MnSOD is a legitimate Sirt3 deacetylation target, an in vitro SIRT3 deacetylation assay was performed. IPed, purified MnSOD was mixed without or with purified SIRT3 with 1 mM NAD+, separated, and immunoblotted with an anti-acetyl, anti-SIRT3, or anti-MnSOD antibody. These experiments showed that Sirt3 decreased MnSOD acetylation (Figure 3E, lane 1 versus 2), and removal of NAD+ (lane 3) or the addition of nicotinamide (lane 4) prevented the deacetylation of MnSOD, suggesting that SIRT3 directly deacetylates MnSOD in vitro. Finally, these experiments were repeated using a specific anti-MnSOD lysine 122 antibody, showing that lysine 122 is deacetylated in vitro by SIRT3 (Figure 3F).

SIRT3 Interacts with MnSOD

Since Sirt3 deacetylates MnSOD, it seemed reasonable to propose that these two proteins might physically interact. As such, HCT116 cells were used that have been genetically altered to overexpress a myc-tagged wild-type *Sirt3* gene (HCT116$^{myc\text{-}SIRT3WT}$ cells). These cells were lysed and IPed with either an anti-MnSOD or anti-myc antibody. The samples were divided into three equal fractions, separated, and subsequently immunoblotted with an anti-myc (Figure 4A, upper panel), anti-SIRT3 (middle panel), or anti-MnSOD (lower panel) antibody. Reverse IPs were also done with anti-SIRT3 (upper panel) or anti-MnSOD (lower panel) antibodies, demonstrating that endogenous SIRT3 and MnSOD appear to form a protein interaction (Figure 4B). These results suggest a potential physical interaction between Sirt3 and MnSOD. In addition, the HCT116 cells were grown on slides that were subsequently stained with anti-MnSOD, anti-SIRT3, DAPI, and MitoTracker (Figure 4C). The immunohistochemical experiments using the anti-MnSOD and anti-SIRT3 staining were also subsequently merged (Figure 4D) and suggest that the SIRT3 and MnSOD proteins colocalized to each other and to the mitochondria. However, these results also show areas where these proteins do not colocalize, as might be expected, since most enzyme/substrate interactions are highly dynamic and may be very transient.

MnSOD Contains an Evolutionarily Conserved Lysine that Directly Regulates Activity

MnSOD is an old, evolutionarily conserved protein present in almost all species, and as such, if a specific MnSOD lysine is an acetylation target in the regulation of enzymatic activity, then it seems reasonable that this lysine would be conserved in multiple mammalian and nonmammalian species. A BLAST search demonstrated a conserved 13 amino acid motif (GELLEAIK*RDFGS) at amino acid 122 that is conserved in human, murine, bovine, etc. (Figure 5A) as well as at position 121 in *C. elegans*. Interestingly, the MnSOD protein in four primates (Rhesus macaque, *Callithrix jacchus*, common gibbon, and chimpanzee) contains an identical 13 amino acid consensus motif; however, it is located 24 amino acids upstream of the human sequence, and the conserved lysine is present at position 98. The consensus motif is also shifted in multiple nonmammalian species, including *Xenopus tropicalis* and zebrafish, to a slightly different protein location (lysine 124 versus 122) (Figure 5A). Thus, it seems reasonable to propose that this conserved 13 amino acid motif, which has remained roughly intact in multiple species, while in some cases being moved to slightly different locations within the MnSOD protein, suggests that this lysine may be of potentially significant

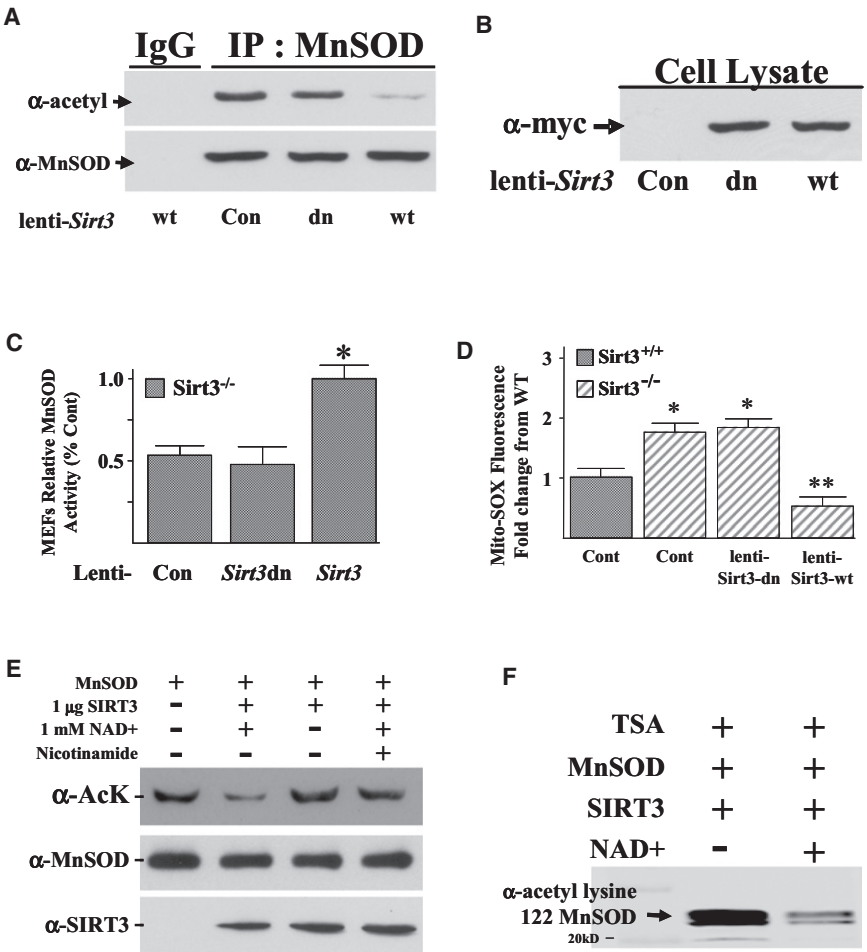

Figure 3. Re-expression of *Sirt3* in Sirt3$^{-/-}$ MEFs Deacetylates MnSOD and Restores SOD Activity

(A) Expression of wild-type but not a deacetylation null mutant of *Sirt3* deacetylates MnSOD. Third-passage Sirt3$^{-/-}$ MEFs were transfected with a control lentivirus, virus expressing a wild-type *Sirt3* (lenti-Sirt3-WT), or deacetylation null gene (lenti-Sirt3-DN). Forty hours after infection, Sirt3$^{-/-}$ MEFs were harvested and mitochondrial extracts were IPed with an anti-MnSOD antibody, separated into two equal fractions, and immunoblotted with either an anti-acetyl or an anti-MnSOD antibody.

(B) The mitochondrial samples above were also separated and immunoblotted with an anti-myc antibody (Santa Cruz Biotechnology, Inc.).

(C) Expression of wild-type but not a deacetylation null mutant *Sirt3* gene increases mitochondrial MnSOD activity. Sirt3$^{-/-}$MEFs were infected with lenti-Sirt3-WT or lenti-Sirt3-DN and assayed for MnSOD activity in 50 mM potassium phosphate buffer. MnSOD activity was determined using an indirect competitive inhibition assay as described in the Experimental Procedures (Spitz and Oberley, 1989). Results in this figure are the mean of at least three separate experiments, and error bars represent one standard deviation. * indicates $p < 0.05$ by t test.

(D) Expression of wild-type but not a deacetylation null mutant *Sirt3* gene decreases mitochondrial superoxide levels. Mitochondrial superoxide levels were determined after infection as described above by the addition of MitoSOX (1 μM) to the cells, followed by incubation for an additional 10 min before being trypsinized and resuspended. Fluorescence was measured via flow cytometry.

(E) SIRT3 directly deacetylates MnSOD in vitro. IPed purified MnSOD was mixed without (lane 1) or with (lanes 2–4) recombinant human SIRT3 with NAD+ (lanes 2 and 4) or nicotinamide (lane 4) and incubated. Samples were separated, followed by immunoblotting with an anti-acetyl antibody. Immunoblotting for SIRT3 and MnSOD were done as internal controls.

(F) IPed, purified MnSOD was mixed in vitro with recombinant human SIRT3 without and with NAD+, separated, and immunoblotted with an anti-K122-MnSOD antibody (Epitomics, Inc.; The Rabbit Monoclonal Antibody Company).

biological and physiological importance. Finally, an examination of the published three-dimensional structure of the MnSOD protein (PDB accession number 1PL4), which is a functional tetramer in vivo, shows that lysine 122 is on the outside of the protein complex in an ideal position to interact with other proteins, such as Sirt3 (Figure S3A).

It has previously been shown that substitution of a lysine with a glutamine mimics an acetylated amino acid state, while substitution with an arginine mimics deacetylation (Li et al., 2007; Schwer et al., 2006). Thus, mutating lysine 122 to arginine would be predicted to mimic a deacetylated lysine, while substitution with a glutamine would be expected to mimic an acetylated lysine (Figure 5B). As such, lenti-MnSOD^{K122} (wild-type), lenti-MnSOD$^{K122\text{-}R}$, lenti-MnSOD$^{K122\text{-}Q}$, and a control virus were used to infect MEFs that have *MnSOD* genetically deleted (MnSOD$^{-/-}$ MEFs) (a kind gift from Prahbat Goswami, University of Iowa). The MnSOD$^{-/-}$ MEFs have previously been shown to have significantly increased mitochondrial superoxide levels as compared to wild-type MEFs (Du et al., 2009).

Infection of the MnSOD$^{-/-}$ MEFs at passage 20 with the various MnSOD lentiviruses resulted in similar levels of cellular exogenous protein (Figure S3B). In addition, infection with the K122-R mutant (lenti-MnSOD$^{K122\text{-}R}$) resulted in increased MnSOD activity (Figure 5C) and decreased mitochondrial superoxide levels (Figure 5D), while the K122-Q mutant displayed the opposite results, when compared to cells infected with the wild-type *MnSOD* lentivirus (Figures 5C and 5D). To make a stronger mechanistic connection between Sirt3 and MnSOD lysine 122, MnSOD$^{-/-}$ MEFs were infected with the wild-type or mutant *MnSOD* viruses and lenti-Sirt3-WT or lenti-Sirt3-DN. These experiments showed that infection of wild-type *Sirt3*, but not the deacetylation null gene, increased MnSOD activity in the MnSOD$^{-/-}$ MEFs expressing wild-type *MnSOD* (Figure 5E, bar 1 versus 2). In contrast, infection with lenti-Sirt3-WT or lenti-Sirt3-DN did not alter the activity of MnSOD in MnSOD$^{-/-}$ MEFs coinfected with either lenti-MnSOD$^{K122\text{-}R}$ or lenti-MnSOD$^{K122\text{-}Q}$. Finally, infection of the MnSOD$^{-/-}$ MEFs with the wild-type- and mutant-MnSOD-expressing lentiviruses did

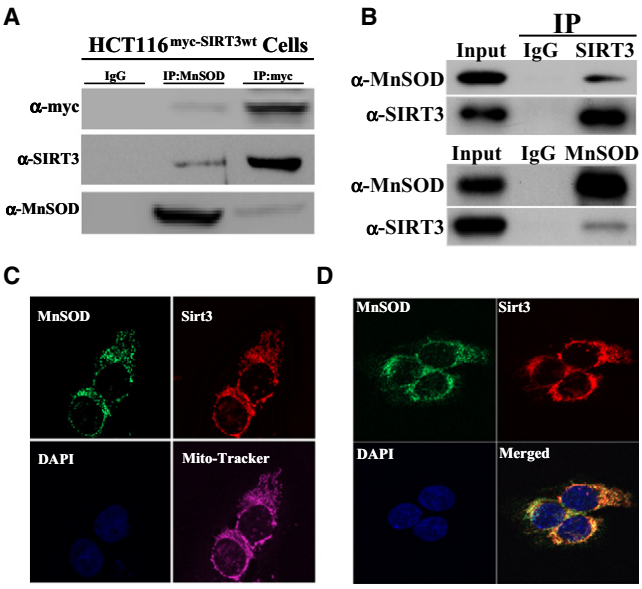

Figure 4. Sirt3 Appears to Interact with MnSOD in the Mitochondria

(A–D) HCT116$^{myc\text{-}Sirt3}$ cells that are genetically altered to overexpress a myc-tagged wild-type *Sirt3* gene (A) and HCT116 cells (B) were harvested and IPed with an anti-SIRT3 or an anti-MnSOD antibody and separated into equal fractions. The samples were resolved and immunoblotted with either an anti-SIRT3 or anti-MnSOD antibody. HCT116 cells were stained with an anti-SIRT3 and anti-MnSOD antibody as well as with DAPI and MitoTracker (C) or with an anti-SIRT3 and anti-MnSOD antibody and DAPI (D), and the images were merged. Representative gels or micrographs for this figure are shown. Results for the panels in this figure are the mean of at least three separate experiments.

not alter cellular H_2O_2 levels (Figure S3C). These results suggest that acetylation of MnSOD lysine 122 directly regulates MnSOD enzymatic dismutase activity.

It has previously been shown that exposure to ionizing radiation (IR) decreases contact inhibition, as measured by increased foci formation, in *MnSOD* knockout MEFs (Du et al., 2009). Infection of the MnSOD$^{K122\text{-}R}$ mutant lentivirus into the MnSOD$^{-/-}$ MEFs (Figure S3B) demonstrated a significant decrease in IR-induced foci formation, while the foci number in the MEFs infected with the MnSOD$^{K122\text{-}Q}$ mutant was identical to the control virus (Figure 5F). Consistent with the idea that MnSOD activity is regulated, at least in part, by acetylation of lysine 122, infection of the MnSOD$^{-/-}$ MEFs with lenti-MnSOD$^{K122\text{-}R}$ also decreased IR-induced mitochondrial superoxide levels (as determined by MitoSOX oxidation) (Figure S3D, lane 5 versus lane 2). In contrast, infection with lenti-MnSOD$^{K122\text{-}Q}$ resulted in MitoSOX oxidation similar to the control cells (lane 4 versus lane 2). These experiments were repeated after coinfection of the MnSOD$^{-/-}$ MEFs with either lenti-Sirt3-WT or lenti-Sirt3-DN. Overexpression of *Sirt3* decreased the number of foci in MnSOD$^{-/-}$ MEFs coinfected with lenti-MnSOD^{K122} (Figure 5G, bar 2 versus 3) to the about same number of foci observed in MEFs infected with lenti-Sirt3-WT or lenti-Sirt3-DN and lenti-MnSOD$^{K122\text{-}R}$ (bar 3 versus 4 and 5). In contrast, infection of lenti-Sirt3-WT or lenti-Sirt3-DN did not change the number of foci in MEFs infected with lenti-MnSOD$^{K122\text{-}R}$ or lenti-MnSOD$^{K122\text{-}Q}$.

Antimycin A, a mitochondrial electron transport chain (Complex III) inhibitor, represents a metabolic stress that is shown to increase superoxide levels (Aykin-Burns et al., 2009). Exposure of MnSOD$^{-/-}$ MEFs to Antimycin A significantly increased superoxide levels (Figure 5H, lane 1), as has been previously shown (Kim et al., 2010). Infection of the MnSOD$^{-/-}$ MEFs with lenti-MnSOD$^{K122\text{-}R}$ (lane 4) and, to a lesser extent, lenti-MnSOD^{K122} (lane 2) prior to exposure to Antimycin A prevented the increase in mitochondrial superoxide levels. In contrast, infection with lenti-MnSOD$^{K122\text{-}Q}$ had no effect on Antimycin A-induced mitochondrial superoxide levels (lane 3) as compared to the control virus-infected cells (lane 1). These results suggest that acetylation of MnSOD regulates MnSOD activity following stress, and this in turn could significantly impact oxidative stress-induced superoxide levels and foci formation, a surrogate marker of in vitro transformation frequency.

MnSOD$^{K122\text{-}R}$ Reverses IR-Induced Increases in Superoxide and Genomic Instability in Sirt3$^{-/-}$ MEFs

The tumor-permissive environment seen in Sirt3$^{-/-}$ animals correlates with the observation that Sirt3$^{-/-}$ MEFs can be immortalized by overexpression of a single oncogene (*Ras* or *Myc*). In addition, exposure of Sirt3$^{-/-}$ MEFs to IR increases mitochondrial superoxide levels and genomic instability (Kim et al., 2010). When Sirt3$^{-/-}$ MEFs were infected with lenti-MnSOD$^{K122\text{-}R}$, but not with lenti-Sirt3$^{K122\text{-}Q}$, immortalization induced by lentivirus-mediated overexpression of *Ras* or *Myc* was inhibited (Table S1). Consistent with this effect being mediated by the activity of MnSOD, infection with lenti-MnSOD$^{K122\text{-}R}$, but not lenti-MnSOD$^{K122\text{-}Q}$, prevented IR-induced increases in steady-state levels of mitochondrial superoxide, as determined by MitoSOX oxidation (Figure 6A), as well as genomic instability, as indicated by IR-induced changes in ploidy (Figure 6B). Western immunoblotting confirmed similar levels of expressed exogenous wild-type and mutant MnSOD protein in the infected Sirt3$^{-/-}$ MEFs (Figure S4A). No change in cellular H_2O_2 levels was observed in the Sirt3$^{-/-}$ MEFs infected with these MnSOD-expressing lentiviruses (Figure S4B).

We have previously shown that Sirt3$^{-/-}$ MEFs immortalized and transformed by infection with *Ras* (referred to as Sirt3$^{-/-}$ Ras cells) exhibit increased growth in soft agar, foci formation, and mitochondrial superoxide levels (Kim et al., 2010). Consistent with the results above, infection with lenti-MnSOD$^{K122\text{-}R}$ and, to a lesser extent, lenti-MnSOD^{K122}, but not lentiMnSOD$^{K122\text{-}Q}$, resulted in decreased growth in soft agar (Figure 6C), decreased foci formation (Figure 6D), and decreased mitochondrial superoxide levels (Figure S4C) in the transformed Sirt3$^{-/-}$ Ras cells. Western immunoblotting confirmed similar levels of expressed exogenous wild-type and mutant MnSOD protein in the infected Sirt3$^{-/-}$ Ras cells (Figure S4D).

In Vivo Liver MnSOD Activity, MnSOD Acetylation, and Radiosensitivity in the Sirt3$^{-/-}$ Mice

The results above suggest that acetylation of MnSOD may alter in vivo responses to radiation exposure. In order to test this hypothesis, Sirt3$^{+/+}$ and Sirt3$^{-/-}$ mice were exposed to 2 Gy of whole-body IR on 2 consecutive days, and liver mitochondria

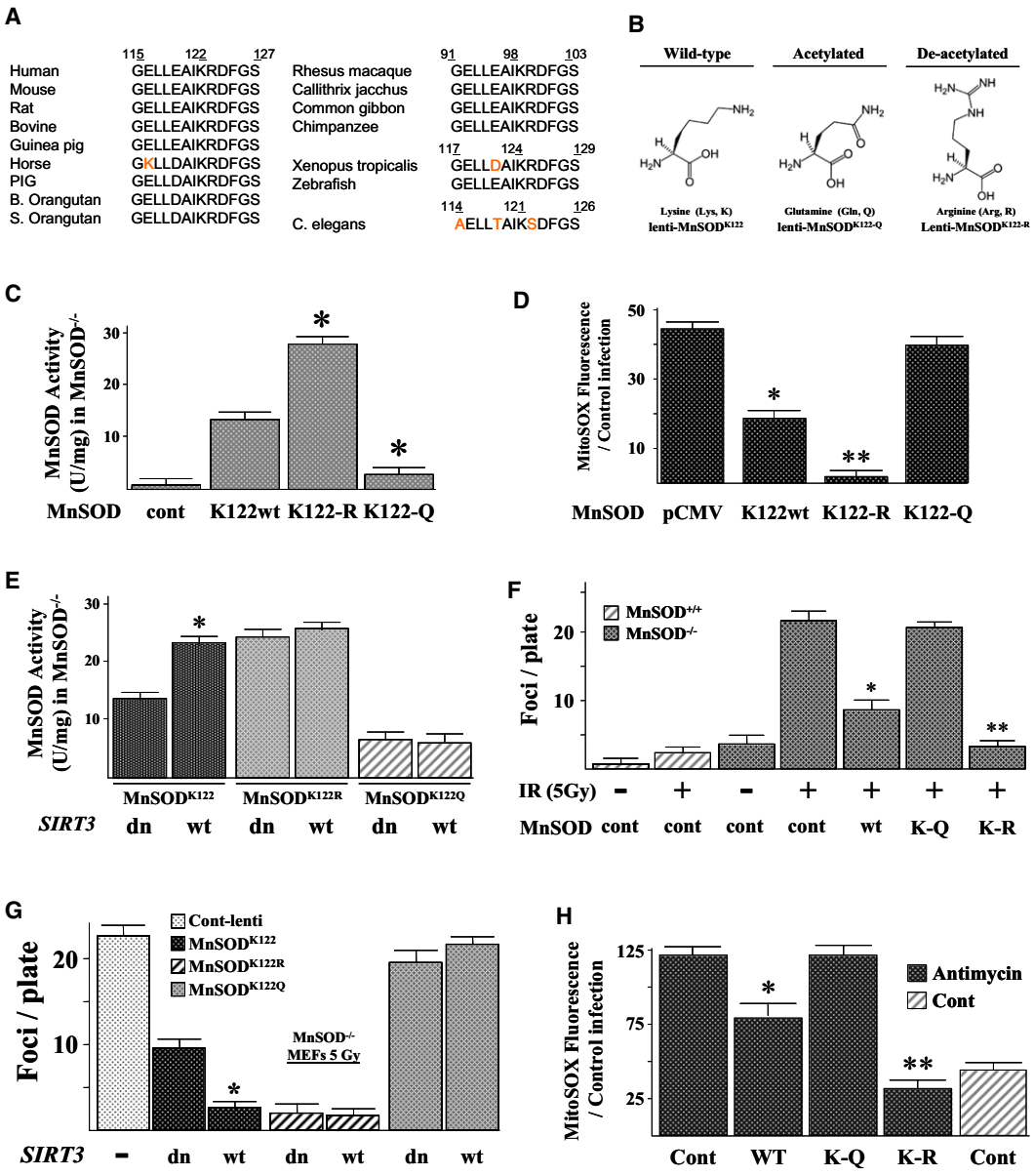

Figure 5. MnSOD Contains an Evolutionarily Conserved Lysine Residue that Regulates SOD Activity

(A) Multiple species contain a potentially reversibly acetylated lysine residue. The MnSOD protein sequence from multiple species was BLASTed based on the reversibly acetylated lysine located at amino acid 122 in mice. A 13 amino acid motif (GELLEAIK*RDFGS) was identified that is present in multiple species.

(B) Substitution of a lysine with a glutamine (Q) mimics an acetylated amino acid state, while substitution with an arginine (R) mimics a deacetylated amino acid state (Li et al., 2007; Schwer et al., 2006).

(C) MnSOD lysine acetylation status directs dismutase activity. MnSOD$^{-/-}$ MEFs were infected with a control lentivirus or lenti-MnSOD^{WT}, lenti-MnSOD^{K122-Q}, or lenti-MnSOD^{K122-R}. Twenty-four hours after infection, MnSOD activity was determined as outlined above (Figure 3 legend).

(D) Mitochondrial superoxide levels are decreased in cells overexpressing a *MnSOD*$^{K122-R}$ mutant gene. MnSOD$^{-/-}$ MEFs were infected with the various MnSOD lentiviruses, and superoxide levels were determined as described above.

(E) MnSOD$^{-/-}$ MEFs were infected with the wild-type and mutant MnSOD lentiviruses with either lenti-Sirt3-WT or lenti-Sirt3-DN and assayed for MnSOD activity.

(F) The MnSOD^{K122-R} mutant decreases IR-induced contact inhibition in the *MnSOD* knockout MEFs. MnSOD$^{-/-}$ MEFs were infected with the MnSOD lentiviruses, plated at 1 × 10^6/100 mm dish, and exposed to 5 Gy IR, followed by long-term culture (28 days), staining with crystal violet, and measurement of foci formation.

(G) MnSOD$^{-/-}$ MEFs were infected with the wild-type and mutant MnSOD lentiviruses with either lenti-Sirt3-WT or lenti-Sirt3-DN and measured for foci formation as above.

(H) Mitochondrial superoxide levels in MnSOD$^{-/-}$ MEFs exposed to Antimcyin A are decreased by infection with lenti-MnSOD^{K122-R}; Sirt3$^{-/-}$ MEFs were treated with 5 μM of Antimycin A for 3 hr, and mitochondrial superoxide levels were determined as described above. Results for all the panels in this figure are the mean of at least three separate experiments, and error bars represent one standard deviation. * indicates $p < 0.05$ and ** indicates $p < 0.01$ by t test.

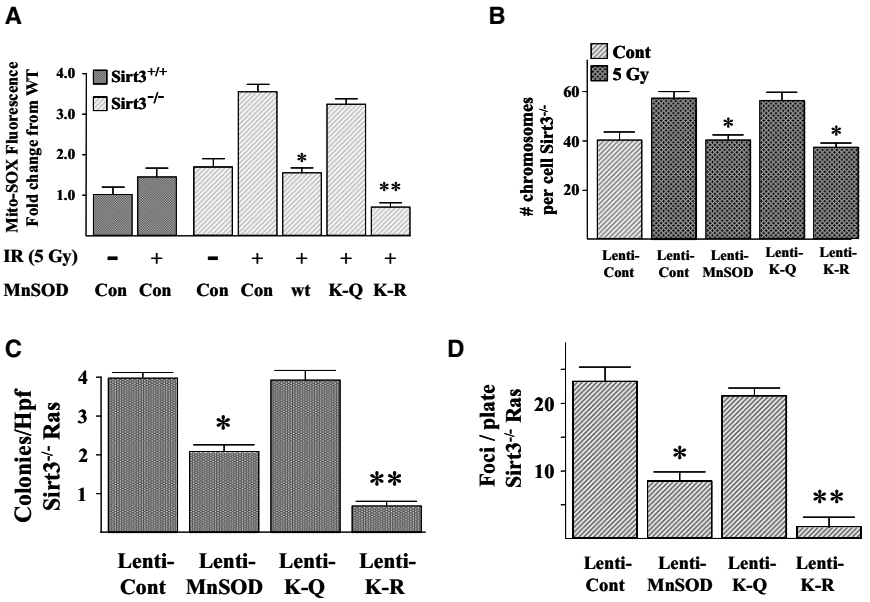

Figure 6. The MnSOD^{K122-R} Mutant Reverses the Increase in IR-Induced Superoxide Levels and Genomic Instability in the Primary or *Ras*-Transformed Sirt3$^{-/-}$ MEFs

(A) Wild-type and Sirt3$^{-/-}$ MEFs were exposed to 5 Gy IR, and mitochondrial superoxide levels were determined by the addition of MitoSOX (1 μM) to the cells.

(B) The MnSOD^{K122-R} mutant prevents aneuploidy in *Sirt3* knockout MEFs exposed to IR. Sirt3$^{-/-}$ MEFs were infected with a control lentivirus or lenti-MnSOD^{WT}, lenti-MnSOD^{K122-Q}, or lenti-MnSOD^{K122-R} and exposed to 5 Gy IR. Whole-mount chromosomes were counted in a blinded fashion. Bars show the mean chromosome number per cell from 100 separate counts.

(C and D) The MnSOD^{K122-R} mutant reverses the transformed phenotype in Sirt3$^{-/-}$ MEFs infected with *Ras*. The transformed Sirt3$^{-/-}$ Ras cells were infected with the *MnSOD* lentiviruses outlined above, and growth in soft agar (C) and spontaneous foci formation (D) were determined as described above. For growth in soft agar, Sirt3$^{-/-}$ Myc/Ras cells were seeded, and colonies were stained with methylene blue after 12 days and counted. Results for all panels in this figure are the mean of at least three separate experiments, and error bars represent one standard deviation. * indicates $p < 0.05$ and ** indicates $p < 0.01$ by t test.

were harvested 24 hr following the second exposure to radiation. These experiments showed a significant IR-induced increase in liver MnSOD activity (Figure 7A) as well as a decrease in lysine 122 MnSOD acetylation (Figures 7B and S5A) in liver mitochondria of Sirt3$^{+/+}$ animals. In contrast, no change in MnSOD activity or lysine acetylation was observed in the liver mitochondria isolated from IR-exposed Sirt3$^{-/-}$ mice (Figures 7A and 7B). Total mitochondrial MnSOD immunoreactive protein levels in the irradiated and control groups were identical (Figure S5B). These results support the hypothesis that Sirt3$^{-/-}$ liver mitochondria lack the capacity to induce MnSOD activity in response to IR because of an inability to deacetylate MnSOD.

If *Sirt3* knockout mice are unable to induce MnSOD activity in response to IR, then it seems reasonable to hypothesize that this loss of the ability to induce a potentially protective response could result in enhanced IR-induced liver damage. As such, livers from Sirt3$^{+/+}$ and Sirt3$^{-/-}$ mice exposed to 2 Gy of radiation on 2 consecutive days were harvested at 24 hr. Histological examination of the irradiated *Sirt3* knockout mice exposed to IR demonstrated marked periportal to midzonal hepatocellular swelling, with dilation of the cytoplasm by clear space, as well as poorly defined vacuoles (Figure 7C). Hepatocellular swelling in the irradiated Sirt3$^{-/-}$ mice livers was significantly more severe as compared to the irradiated Sirt3$^{+/+}$ or the control Sirt3$^{+/+}$ and Sirt3$^{-/-}$ mice (Figure 7D). Liver sections processed with osmium tetroxide (stains lipid in fixed tissue) demonstrated minimal to no lipid vacuoles in the swollen hepatocytes of Sirt3$^{-/-}$ mice (Figure S5C, top panels). In addition, liver sections from irradiated Sirt3$^{-/-}$ mice stained with periodic acid-Schiff (PAS) (stains glycogen) demonstrated mild to moderate cytoplasmic glycogen with poorly defined clear spaces (Figure S5C, bottom panels). This histology displays some characteristics similar, at least in part, to those observed in microvesicular steatosis that is associated with mitochondrial dysfunction (Araya et al., 2006). Interestingly, the risk factors for steatosis include diabetes mellitus, protein malnutrition, and obesity (Araya et al., 2006), all of which have been associated with abnormalities of sirtuin function (Finkel et al., 2009).

When the livers from these mice were stained with markers for apoptosis, the *Sirt3* knockout mice exposed to irradiation demonstrated significantly more apoptosis then the irradiated wild-type mice, as well as the control Sirt3$^{+/+}$ and Sirt3$^{-/-}$ mice, as measured by TUNEL assay (Figure 7E) or staining with antibodies to cleaved caspase-3 (Figure S5D). This result is consistent with the increased cellular damage and the membrane-bound vacuoles observed in the H&E staining (Tolman and Dalpiaz, 2007).

Control and irradiated Sirt3$^{+/+}$ and Sirt3$^{-/-}$ livers were also stained with an anti-nitrotyrosine antibody as a marker for increased protein damage caused by intracellular reactive oxygen/nitrogen species, specifically $ONOO^-$, a reaction product of nitric oxide and superoxide (Kim et al., 2010). *Sirt3* knockout mouse liver cells exhibited increased anti-nitrotyrosine staining (Figure 7F), as compared the Sirt3$^{+/+}$ samples (quantified in Figure S5E, $p < 0.05$), and there was a very significant difference between the Sirt3$^{+/+}$ and Sirt3$^{-/-}$ irradiated liver samples (bar 2 versus 4, $p < 0.01$). These results suggest an oxidative stress-permissive phenotype in liver cells lacking *Sirt3* that becomes more evident upon IR-induced oxidative stress.

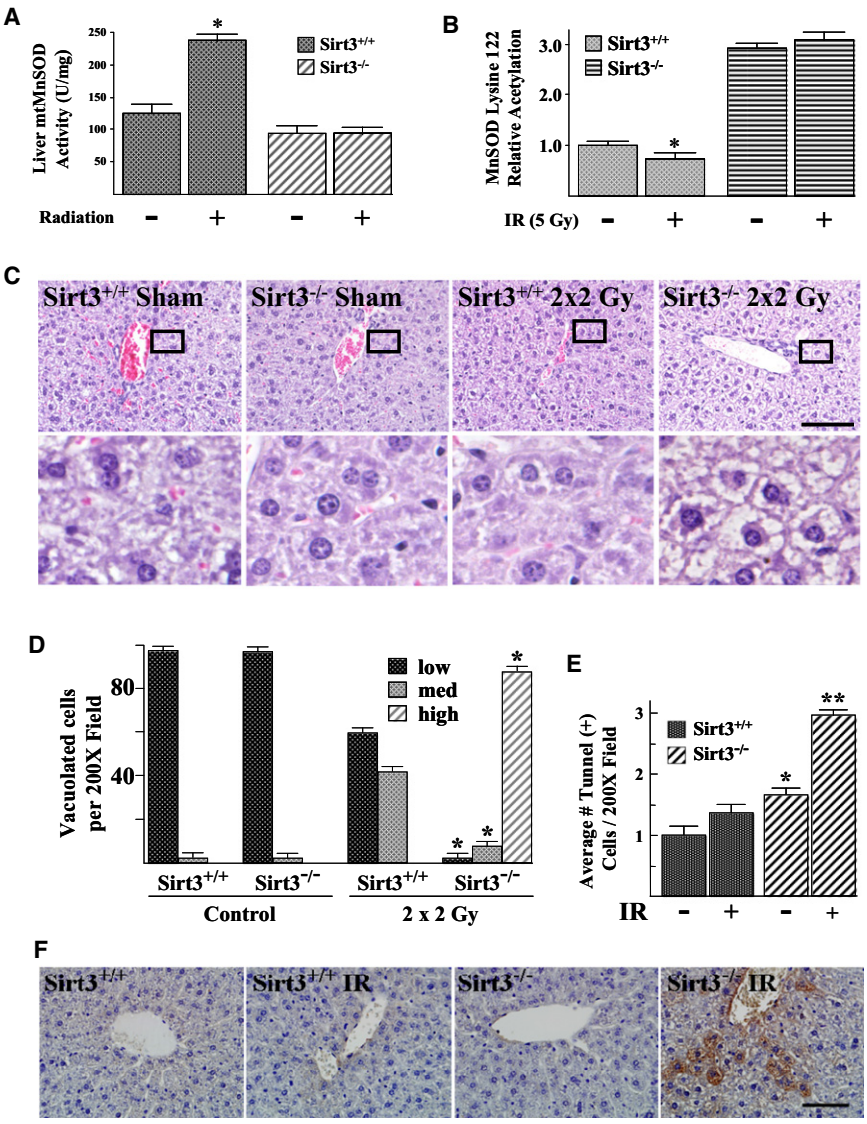

Figure 7. MnSOD Dismutase Activity, Lysine 122 Acetylation, and the Cellular Metabolic and Damage/Cytotoxic Response Are Altered by IR

(A) Sirt3$^{+/+}$ and Sirt3$^{-/-}$ mice at 12 weeks were exposed to ionizing radiation (2 Gy on 2 consecutive days) or sham treated every 24 hr. Livers were harvested 24 hr postexposure and mitochondria were isolated. MnSOD activity in MEFs was measured via a competitive inhibition assay as described (Spitz and Oberley, 1989). Activity data for MnSOD are presented as units of SOD activity per milligram of protein.

(B) Mitochondrial extracts from above were analyzed for acetylation of MnSOD lysine 122 via mass spectrometry. Results are presented as fold change from the untreated, wild-type mouse livers.

(C) Sirt3$^{-/-}$ mouse livers exposed to IR exhibit marked cytoplasmic vacuolation of periportal to midzonal hepatocytes. The wild-type and Sirt3$^{-/-}$ livers without and with exposure to IR were H&E stained and scored for degree of hepatocellular cytoplasmic vacuolation—low, medium, and high—by a pathologist. Representative micrographs are shown. Scale bar = 80 μm.

(D) Quantification of the H&E for liver cells. Liver cells were scored as follows: low, no detectable cytoplasmic vacuolation; med, moderate dilation of the cytoplasm by clear space primarily affecting periportal hepatocytes; high, severe dilation of the cytoplasm by clear space and poorly defined clear vacuoles primarily affecting periportal to midzonal hepatocytes.

(E) Apoptosis was determined in the Sirt3$^{+/+}$ and Sirt3$^{-/-}$ livers exposed to IR. Apoptotic cells were identified in liver sections by TUNEL assay. Sections were scored by a pathologist blinded to the groupings. TUNEL-positive cells were counted in ten randomly selected 200× fields per liver section. Results in this figure are reported as the average number of positive cells per field. Data are presented as the average ± SD. * indicates $p < 0.05$ and ** indicates $p < 0.01$.

(F) Irradiated Sirt3$^{-/-}$ mouse liver cells exhibit increased anti-nitrotyrosine IHC staining. Liver tissues from wild-type and Sirt3$^{-/-}$ mice were stained with an anti-nitrotyrosine antibody (StressMarq Biosciences Inc.; Victoria, British Columbia, Canada). A representative micrograph is shown. Scale bar = 80 μm. See Figure S5E for quantification.

DISCUSSION

We have previously demonstrated that Sirt3 is an in vitro and in vivo TS protein and that the knockout mice spontaneously develop well-differentiated, ER/PR-positive mammary tumors (Kim et al., 2010). In addition, SIRT3 protein levels are decreased in human breast cancers as well as in several other human malignancies. These results identified Sirt3 as a genomically expressed, mitochondrially localized TS, and cells lacking *Sirt3* may be a useful in vivo model to investigate the subtype of breast cancer observed in postmenopausal or older women.

One intriguing finding from our previous work was that cells lacking *Sirt3* exhibited altered mitochondrial metabolism, as exhibited by increased mitochondrial superoxide levels during stress. These results suggested a connection between the increase in superoxide and the *Sirt3* knockout mouse tumor-permissive phenotype. However, one outstanding question from this previous work involved the observation that MnSOD transcription, via FOXO3a acetylation, was not decreased until 1 year—roughly the same time that the mammary tumors were first observed in the *Sirt3* knockout mice. Thus, while the connection between the MnSOD and increased mitochondrial superoxide seemed strong, the mechanism appeared to be more complex than a decrease in FOXO3a-driven MnSOD transcription (Kim et al., 2010). Thus, additional wild-type and *Sirt3* knockout mouse colonies were established and followed to more rigorously investigate the connection between superoxide levels and MnSOD as an early carcinogenic event in the *Sirt3*

knockout mouse tumor-permissive phenotype. These results suggested a second potential mechanism for Sirt3 regulation of MnSOD activity that is independent of *MnSOD* expression and potentially related to posttranslational modification involving acetylation.

The connection between mitochondrial damage and carcinogenesis is well established; however, the mechanism appears to be complex (Singh, 2006; Wallace, 2005). In addition, it has been suggested that the mitochondria play a role in radiation-induced malignancies, but the specific molecular steps are not completely understood (Du et al., 2009). One proposed mechanism involves the accumulation of mitochondrial ROS; these reactive molecules can damage numerous cellular processes, creating an environment permissive for genomic instability as well as carcinogenesis (Oberley, 2005). Since Sirt3 is the primary mitochondrial deacetylase, we hypothesized that the increase in mitochondrial superoxide levels in *Sirt3* knockout mice and MEFs exposed to stress may be due to aberrant acetylation and regulation of MnSOD enzymatic activity.

Our results identify MnSOD amino acid 122 as a reversibly acetylated lysine residue that is deacetylated by 36 hr of fasting, and MnSOD acetylation is significantly increased and enzymatic activity decreased in Sirt3$^{-/-}$ cells. In addition, MnSOD is deacetylated by Sirt3, suggesting that mitochondrial acetylation plays a role, at least in part, in regulation of MnSOD function. This idea was validated by a pair of MnSOD mutants that demonstrated increased activity when lysine 122 was changed to arginine (to mimic the deacetylated state). MnSOD$^{K122\text{-}R}$ also prevented IR-induced foci formation in MnSOD$^{-/-}$ cells and immortalization of Sirt3$^{-/-}$ MEFs by a single oncogene, as well as IR-induced genomic instability and loss of contact inhibition.

Finally, we show in vivo that IR induces deacetylation of MnSOD and increased enzymatic activity in irradiated wild-type mouse liver mitochondria, but not in liver mitochondria of the *Sirt3* knockout mice. While it is tempting to suggest this IR-induced damage-permissive phenotype is primarily due to changes in MnSOD activity, it seems likely that other Sirt3 deacetylation targets may also play a role in this histological and biochemical phenotype. This idea would fit the well-established data that IR-induced damage and cytotoxicity is a multifactorial process involving several cellular proreparative pathways, including redox scavenging, DNA repair, and stress-responding proteins. Taken together, the in vivo and in vitro results suggest MnSOD enzymatic activity is regulated by acetylation during stress and that Sirt3 regulates acetylation under specific conditions associated with neoplastic transformation, including IR-induced cellular damage.

A fundamental paradigm in biology is the presence of intracellular redox-sensing proteins that recognize specific cellular conditions and initiate posttranslational signaling cascades (Slane et al., 2006), and these pathways activate the cellular machinery that maintains cellular homeostasis. The most common example of this is the cytoplasmic activation of kinases that phosphorylate a series of downstream targets in response to different environmental conditions, thereby minimizing any potentially permanent cellular detrimental effects (Slane et al., 2006). In this regard, lysine acetylation has recently emerged as an important and perhaps primary posttranslational modification employed to regulate mitochondrial proteins (Lombard et al., 2007).

The results presented above support this hypothesis and, together with recent findings (Kim et al., 2010), suggest that mitochondrial sirtuins, including Sirt3, may function as fidelity proteins whose loss of function may result in a damage-permissive phenotype that leads to neoplastic transformation. The results presented above also suggest that the superoxide scavenging enzymatic function of MnSOD is regulated by changes in specific lysine acetylation. The connection between MnSOD and carcinogenesis, as well as tumor cell resistance to anticancer agents, is significant; however, the mechanism of action appears to be complex (Oberley, 2005; Aykin-Burns et al., 2009). The current work represents a paradigm shift in our understanding of the posttranslational regulation of MnSOD enzymatic function and the mechanism of its role in responses to stress. Finally, since Sirt3 is proposed to sense nutrient deprivation and oxidative stress, it also seems logical that exposure to IR, which has previously been shown to induce both oxidative stress and mitochondrial damage (Slane et al., 2006), would activate Sirt3 as a signaling pathway to protect against persistent IR-induced metabolic stress and normal tissue damage.

EXPERIMENTAL PROCEDURES

Cell Lines

MEFs were isolated from E14.5 isogenic *Sirt3*$^{+/+}$ and *Sirt3*$^{+/+}$ mice and maintained in a 37°C incubator with 5% CO_2 and 6% oxygen. MEFs and HCT-116 were cultured in McCoy's 5A media, containing 10% heat-inactivated (56°C, 30 min) FBS. Sirt3$^{+/+}$ or Sirt3$^{-/-}$ MEFs (Kim et al., 2010) were infected at P3 with lentivirus expressing either *Myc*, *Ras*, or *MnSOD* made by Applied Biological Materials, Inc. (Richmond, British Columbia, Canada), and pooled, selected cells were used for all experiments. For lentiviral infections, MEFs were infected with 5 moi of virus.

IP and Immunoblot Analysis

IP with anti-MnSOD and anti-Sirt3 antibodies and the subsequent western analyses were done as previously described (Kim et al., 2010). The control for these IP experiments is normalized to rabbit IgG. In addition, the IPed MnSOD samples were divided into equal fractions, separated, and blotted with anti-acetyl or anti-MnSOD antibodies. Blots were incubated with horseradish peroxidase secondary antibody, using ECL (Amersham Biosciences; Piscataway, NJ), and visualized in a Fuji Las-3000 darkbox (FujiFilm Systems; Stamford, CT).

Statistical Analysis

Data were analyzed by Student's t test, and results were considered significant at $p < 0.05$. Results are presented as mean ± SD.

MnSOD Activity

MnSOD activity was analyzed in cell homogenates prepared on ice in 50 mM potassium phosphate buffer (Spitz and Oberley, 1989). This assay is based on the competition between MnSOD and an indicator molecule for superoxide production from xanthine and xanthine oxidase, in the presence of 5 mM NaCN to inhibit CuZnSOD activity (Spitz and Oberley, 1989). See Supplemental Experimental Procedures.

Measurement of Mitochondrial Superoxide Levels

Superoxide production was determined as described (Kim et al., 2010) by measuring MitoSOX (1 μM) oxidation in cells that were cultured as described above and incubated for an additional 10 min before being trypsinized, resuspended, and measured by flow cytometry (see Supplemental Information).

Liver samples were used to determine in vivo superoxide levels as previously described (Kim et al., 2010).

Cell Foci, Colony Formation, and Soft Agar Assays

For foci formation assays, cells were plated onto a 10 cm plate and grown to confluence, with medium replaced every 3 days for 28 days. All results for these experiments are the mean of at least three separate experiments. For the soft agar colony formation assay, 4000 cells were plated in 2 ml of 0.4% agar in growth medium over a 3 ml base layer of agar, also in growth medium. Each culture was topped with 1–2 ml of medium every 3–5 days. After 12 days, colonies were stained with methylene blue. The colonies (>0.5 mm size) were counted after 2 weeks under a light microscope.

Chromosome Analysis

MEFs were exposed at passage four to irradiation and harvested after 72 hr. Whole-mount chromosomes were counted in a blinded fashion. Individual spreads were deemed countable if all chromosomes were clearly defined and clearly visible within a single cytoplasm, as previously described (Kim et al., 2010).

Catalase Enzymatic Activity

Catalase activity was determined as described (Slane et al., 2006). Cell extracts containing 100 μg protein were combined with 30 mM H_2O_2 (Fisher Scientific; Suwanee, GA) in 1 ml of 50 mM potassium phosphate buffer (pH 7.0). H_2O_2 disappearance was measured at 240 nm for 120 s and recorded over 15 s intervals. Catalase enzymatic activity was expressed in k units per microgram protein per second (k units/μg/s): $k = 1/60 \times \ln(A0/A60)$, where A0 is the initial absorbance and A60 is the absorbance at 60 s.

Liver Histopathology Examination, TUNEL Assay, and Cleaved Caspase-3 IHC

Liver sections were fixed in 10% neutral buffered formalin. Fixed tissues were then processed, paraffin embedded, and sectioned at 4 μm. Sections were stained with H&E or PAS reagent (for glycogen evaluation). H&E slides were scored in a blinded fashion for severity of hepatocellular vacuolation. The vacuolar change, when present, was focused in periportal to midzonal hepatocytes; therefore, scoring was based on an average of three periportal areas per liver section. For each periportal area, 100 hepatocytes were counted and given a vacuolar severity score of low, medium, or high. Low vacuolar change was characterized by mild, poorly defined cytoplasmic vacuolation consistent with glycogen accumulation. Hepatocytes with medium or high vacuolation were moderately to markedly enlarged due to dilation of the cytoplasm by clear space and few poorly defined clear vacuoles. Osmium tetroxide staining for lipid (to identify hepatocellular lipid vacuoles) was performed on formalin-fixed tissues. Formalin-fixed tissues (3 mm) were placed in potassium dichromate/osmium tetroxide (5%/2%) for 7 hr, followed by a 2 hr tap water rinse. Tissue sections were then routinely processed, paraffin embedded, and sectioned.

TUNEL assay was performed using the ApopTag Peroxidase ISOL Apoptosis Detection Kit (Millipore; Billerica, MA) according to the manufacturer's instructions. Apoptosis was detected by IHC for cleaved caspase-3 on formalin-fixed, paraffin-embedded liver tissues. Cleaved caspase-3 antibody, which is indicative of activated caspase-3 (rabbit monoclonal 1:50, Cell Signaling Technologies; Danvers, MA), was applied for 1 hr. Following several rinses, secondary antibody (Rabbit Envision HRP System, DAKO; Carpinteria, CA) and chromogen (Rabbit Envision HRP System reagents, DAB Plus, and DAB Enhancer; DAKO) kits were applied as per the manufacturer's instructions. TUNEL and caspase-3 staining were quantified by counting positive cells per 200× field. A total of 10–200× fields were counted, and means of these counts were calculated for further statistical analysis.

SUPPLEMENTAL INFORMATION

Supplemental Information includes Supplemental Experimental Procedures, Supplemental References, six figures, and one table and can be found with this article online at doi:10.1016/j.molcel.2010.12.013.

ACKNOWLEDGMENTS

D.G. is supported by 1R01CA152601-01 from the NCI, BC093803 from the DOD, and SPORE P50CA98131. D.R.S., A.K.O., and M.C.C. are supported by grants from the NIH and DOE (R01CA133114, T32CA078586, P30CA086862, and DE-SC0000830). J.D.P. is supported by F30AG030839. We thank Melissa Stauffer of Scientific Editing Solutions for editorial assistance.

Received: July 13, 2010
Revised: October 10, 2010
Accepted: December 6, 2010
Published: December 21, 2010

REFERENCES

Ahn, B.H., Kim, H.S., Song, S., Lee, I.H., Liu, J., Vassilopoulos, A., Deng, C.X., and Finkel, T. (2008). A role for the mitochondrial deacetylase Sirt3 in regulating energy homeostasis. Proc. Natl. Acad. Sci. USA *105*, 14447–14452.

Araya, Q.A.V., Valera, M.J.M., Contreras, B.J., Csendes, J.A., Díaz, J.J., Burdiles, P.P., Rojas, C.J., Maluenda, G.F., Smok, S.G., and Poniachik, T.J. (2006). [Glucose tolerance alterations and frequency of metabolic syndrome among patients with non alcoholic fatty liver disease]. Rev. Med. Chil. *134*, 1092–1098.

Aykin-Burns, N., Ahmad, I.M., Zhu, Y., Oberley, L.W., and Spitz, D.R. (2009). Increased levels of superoxide and H2O2 mediate the differential susceptibility of cancer cells versus normal cells to glucose deprivation. Biochem. J. *418*, 29–37.

Du, C., Gao, Z., Venkatesha, V.A., Kalen, A.L., Chaudhuri, L., Spitz, D.R., Cullen, J.J., Oberley, L.W., and Goswami, P.C. (2009). Mitochondrial ROS and radiation induced transformation in mouse embryonic fibroblasts. Cancer Biol. Ther. *8*, 1962–1971.

Finkel, T., Deng, C.X., and Mostoslavsky, R. (2009). Recent progress in the biology and physiology of sirtuins. Nature *460*, 587–591.

Kim, H.S., Patel, K., Muldoon-Jacobs, K., Bisht, K.S., Aykin-Burns, N., Pennington, J.D., van der Meer, R., Nguyen, P., Savage, J., Owens, K.M., et al. (2010). SIRT3 is a mitochondria-localized tumor suppressor required for maintenance of mitochondrial integrity and metabolism during stress. Cancer Cell *17*, 41–52.

Li, X., Zhang, S., Blander, G., Tse, J.G., Krieger, M., and Guarente, L. (2007). SIRT1 deacetylates and positively regulates the nuclear receptor LXR. Mol. Cell *28*, 91–106.

Lombard, D.B., Alt, F.W., Cheng, H.L., Bunkenborg, J., Streeper, R.S., Mostoslavsky, R., Kim, J., Yancopoulos, G., Valenzuela, D., Murphy, A., et al. (2007). Mammalian Sir2 homolog SIRT3 regulates global mitochondrial lysine acetylation. Mol. Cell. Biol. *27*, 8807–8814.

Oberley, L.W. (2005). Mechanism of the tumor suppressive effect of MnSOD overexpression. Biomed. Pharmacother. *59*, 143–148.

Onyango, P., Celic, I., McCaffery, J.M., Boeke, J.D., and Feinberg, A.P. (2002). SIRT3, a human SIR2 homologue, is an NAD-dependent deacetylase localized to mitochondria. Proc. Natl. Acad. Sci. USA *99*, 13653–13658.

Revollo, J.R., Grimm, A.A., and Imai, S. (2004). The NAD biosynthesis pathway mediated by nicotinamide phosphoribosyltransferase regulates Sir2 activity in mammalian cells. J. Biol. Chem. *279*, 50754–50763.

Schwer, B., North, B.J., Frye, R.A., Ott, M., and Verdin, E. (2002). The human silent information regulator (Sir)2 homologue hSIRT3 is a mitochondrial nicotinamide adenine dinucleotide-dependent deacetylase. J. Cell Biol. *158*, 647–657.

Schwer, B., Bunkenborg, J., Verdin, R.O., Andersen, J.S., and Verdin, E. (2006). Reversible lysine acetylation controls the activity of the mitochondrial enzyme acetyl-CoA synthetase 2. Proc. Natl. Acad. Sci. USA *103*, 10224–10229.

Sherr, C.J., and McCormick, F. (2002). The RB and p53 pathways in cancer. Cancer Cell *2*, 103–112.

Singh, K.K. (2006). Mitochondria damage checkpoint, aging, and cancer. Ann. N Y Acad. Sci. *1067*, 182–190.

Slane, B.G., Aykin-Burns, N., Smith, B.J., Kalen, A.L., Goswami, P.C., Domann, F.E., and Spitz, D.R. (2006). Mutation of succinate dehydrogenase subunit C results in increased O2.-, oxidative stress, and genomic instability. Cancer Res. *66*, 7615–7620.

Spitz, D.R., and Oberley, L.W. (1989). An assay for superoxide dismutase activity in mammalian tissue homogenates. Anal. Biochem. *179*, 8–18.

Tolman, K.G., and Dalpiaz, A.S. (2007). Treatment of non-alcoholic fatty liver disease. Ther Clin Risk Manag *3*, 1153–1163.

Wallace, D.C. (2005). Mitochondria and cancer: Warburg addressed. Cold Spring Harb. Symp. Quant. Biol. *70*, 363–374.